

## A FIXED-MESH METHOD FOR GENERAL MOVING OBJECTS

Gengsheng Wei  
Flow Science, Inc.  
August, 2005

A fixed-mesh method for general moving objects in fluid flow was developed and implemented into *FLOW-3D*<sup>®</sup>. A general moving object (GMO) is a rigid body with any type of six-degrees-of-freedom, fixed-point and fixed-axis motion which can be either user-prescribed or dynamically coupled with fluid flow. The method allows for multiple independently general moving objects. Equations of motion for rigid body are solved for coupled motion. Area and volume fractions are used to represent the objects in the fixed-grid at every time step to describe time-variation of object locations and orientations. Continuity and momentum equations for fluid and scalar transport equations are modified to account for the effects of object motion. Good agreement was achieved between computational and theoretical/experimental results in several application cases.

---

### 1. Introduction

There are many engineering practices in which objects move in fluid. Conventional CFD methods for moving objects are mainly based on moving and deforming mesh techniques (Crank 1984, Finlayson, 1992). They have the limitations that either distance between moving objects cannot be too small or they fail when mesh distortion become too severe. Although remeshing may help overcome the limitations, it requires repeated automatic mesh regeneration, and thus can be prohibitively expensive for application.

*FLOW-3D*<sup>®</sup> has been using its unique FAVOR<sup>™</sup> technique to describe geometric objects in a computational domain with concepts of area fraction (AF) and volume fraction (VF) in rectangular meshes (Hirt and Sicilian, 1985). The VF is defined as the ratio of the open volume to the total volume in a mesh cell, and three AFs (AFR, AFB, AFT) are defined respectively at the three cell faces in the increasing cell-index direction as the ratio of the open area to the total area. The FAVOR<sup>™</sup> technique deals with complex geometries by introducing effects of AF and VF into the conservation equations. Previously, in *FLOW-3D*<sup>®</sup>, Sicilian (1990) developed a method for prescribed piston motion along the z-direction. This method has been successfully applied to many engineering problems, but its area of application is quite limited. Later Ditter and Hirt (1993) developed a “phantom” component method for axisymmetric objects under prescribed rotation about a fixed axis. This method assumes that the rotating object does not block fluid flow but transfers momentum to fluid in the form of a linear function of the relative velocity between the moving object and the fluid. Although successful applications of the method have been achieved, an empirical momentum-transfer coefficient is required, which must be adjusted from case to case.

In this work, a fixed-mesh method for general moving objects (GMO model) based on the FAVOR<sup>™</sup> technique is developed and implemented in *FLOW-3D*<sup>®</sup>. Multiple

moving objects can be modeled within the same computational domain, each having either a six-degrees-of-freedom (DOF), or fixed-point, or fixed-axis motion, either user-prescribed or dynamically coupled with fluid flow. At each time step, AF and VF are calculated to describe object's location in a fixed-rectangular mesh. Hydraulic, gravitational, environmental and control forces and torques are calculated, and equations of motion for rigid body are solved explicitly for translational and rotational velocities for each moving object under a coupled motion. The continuity equation is modified with the addition of a source term to account for fluid displacement. Wall shear terms in the momentum equations are modified to include the effect of moving object boundaries. This method has advantages over the moving and deforming mesh methods because it treats complex moving object geometries very efficiently and conveniently and there is no restriction on closeness between objects. This model works with most physical models and numerical methods in *FLOW-3D*<sup>®</sup>, but some limitations exist. All moving objects must be solid with no porosity. No collision capability between objects has been developed yet. For fixed axis motion, the axis must be parallel to one of the three coordinate axes of the space system. A detailed description of the method and results of several test cases are presented and discussed in the following sections.

## 2. Equations of Motion for Moving Object

For convenience of computation, a body-fixed reference system (“body system”) ( $x'$ ,  $y'$ ,  $z'$ ) is set up for each moving object with its coordinate axes parallel to those of the space system at time  $t = 0$ . If an object motion has six DOF, origin of the body system is set at the object mass center  $G$ . Coordinate transformation between the space system ( $x$ ,  $y$ ,  $z$ ) and the body systems ( $x'$ ,  $y'$ ,  $z'$ ) is

$$\vec{x}_s = [R] \cdot \vec{x}_b + \vec{x}_G, \quad (1)$$

where  $\vec{x}_s$  and  $\vec{x}_b$  are position vectors of a point in space and body systems, respectively,  $\vec{x}_G$  is position vector of the mass center in space system, and  $[R]$  is an orthogonal transformation tensor,

$$[R] = \begin{bmatrix} R_{11} & R_{12} & R_{13} \\ R_{21} & R_{22} & R_{23} \\ R_{31} & R_{32} & R_{33} \end{bmatrix}, \quad (2)$$

where  $R_{ij}R_{jk} = \delta_{ik}$ , and  $\delta_{ik}$  is the Kronecker  $\delta$  symbol. It is a property of  $[R]$  that its inverse and transposed matrices are identical. For a space vector  $\vec{A}$ , the transformation between the space and body systems is

$$\vec{A}_s = [R] \cdot \vec{A}_b, \quad (3)$$

where  $\vec{A}_s$  and  $\vec{A}_b$  denote the  $A$  expressions in space and body systems, respectively.  $[R]$  is calculated by solving

$$\frac{d[R]}{dt} = [\Omega] \cdot [R], \quad (4)$$

where

$$[\Omega] = \begin{bmatrix} 0 & -\Omega_z & \Omega_y \\ \Omega_z & 0 & -\Omega_x \\ -\Omega_y & \Omega_x & 0 \end{bmatrix}, \quad (5)$$

and  $\Omega_x$ ,  $\Omega_y$  and  $\Omega_z$  are the x-, y- and z-components of the angular velocity of the object in space system, respectively.

According to kinematics, general motion of a rigid body can be partitioned into a translational motion and a rotational motion. Velocity of any point on a rigid body is equal to the velocity of an arbitrarily selected base point on the object plus velocity due to the rotation about the base point. It is convenient to select the object mass center as the base point for a 6-DOF motion. Denoting P as a point on the object, its velocity is related to the mass center velocity  $\vec{V}_G$  and angular velocity  $\vec{\omega}$  of the rigid body by

$$\vec{V}_P = \vec{V}_G + \vec{\omega} \times \vec{r}_{P/G}, \quad (6)$$

where  $\vec{r}_{P/G}$  is the distance vector from G to P. The first term on the right-hand side of equation (6) represents translation of the mass center and the second term is the rotation about the mass center. Note that  $\vec{\omega}$  is a property of the moving object and is independent of the choice of the base point. Equations of motion governing the two separate motions are

$$\vec{F} = m \frac{d\vec{V}_G}{dt} \quad (7)$$

$$\vec{T}_G = [J] \cdot \frac{d\vec{\omega}}{dt} + \vec{\omega} \times ([J] \cdot \vec{\omega}), \quad (8)$$

where  $\vec{F}$  is the total force,  $m$  is the rigid body mass,  $\vec{T}_G$  is the total torque about G,  $[J]$  is moment of inertia tensor about G in the body system (“inertia tensor”),

$$[J] = \begin{bmatrix} J_{11} & J_{12} & J_{13} \\ J_{21} & J_{22} & J_{23} \\ J_{31} & J_{32} & J_{33} \end{bmatrix}, \quad (9)$$

The diagonal elements of  $[J]$  are moments of inertia and the others elements are products of inertia, which are expressed as

$$J_{11} = \int (y'^2 + z'^2) dm, \quad J_{22} = \int (x'^2 + z'^2) dm, \quad J_{33} = \int (x'^2 + y'^2) dm, \quad (10)$$

$$J_{12} = J_{21} = -\int x' y' dm, \quad J_{13} = J_{31} = -\int x' z' dm, \quad J_{23} = J_{32} = -\int y' z' dm. \quad (11)$$

If  $x'$ ,  $y'$  and  $z'$  coincide with the principle axes of the object, the products of inertia vanish. To simplify the calculations, equations (7) and (8) are solved in space and body systems, respectively. Component equations of (8) in  $x'$ ,  $y'$  and  $z'$  directions of body system are

$$\begin{aligned} T_{G1} &= J_{11}\dot{\omega}_1 + J_{12}\dot{\omega}_2 + J_{13}\dot{\omega}_3 + \omega_2(J_{31}\omega_1 + J_{32}\omega_2 + J_{33}\omega_3) - \omega_3(J_{21}\omega_1 + J_{22}\omega_2 + J_{23}\omega_3) \\ T_{G2} &= J_{21}\dot{\omega}_1 + J_{22}\dot{\omega}_2 + J_{23}\dot{\omega}_3 + \omega_3(J_{11}\omega_1 + J_{12}\omega_2 + J_{13}\omega_3) - \omega_1(J_{31}\omega_1 + J_{32}\omega_2 + J_{33}\omega_3) \\ T_{G3} &= J_{31}\dot{\omega}_1 + J_{32}\dot{\omega}_2 + J_{33}\dot{\omega}_3 + \omega_1(J_{21}\omega_1 + J_{22}\omega_2 + J_{23}\omega_3) - \omega_2(J_{11}\omega_1 + J_{12}\omega_2 + J_{13}\omega_3) \end{aligned} \quad (12)$$

where  $\omega_i$  and  $\dot{\omega}_i$  ( $i=1, 2, 3$ ) are components of angular velocity and angular acceleration along body-fixed coordinate axes  $x'$ ,  $y'$  and  $z'$ , respectively.

In general, the total force can be divided into several net components,

$$\vec{F} = \vec{F}_g + \vec{F}_h + \vec{F}_c + \vec{F}_{ni} \quad (13)$$

where  $\vec{F}_g$  is the gravitational force,  $\vec{F}_h$  is the hydraulic force which is the net effect of pressure and wall shear forces on the moving object,  $\vec{F}_c$  is the net control force such as propulsive thrust force and axis force to control or restrict the object's motion, and  $\vec{F}_{ni}$  is the net non-inertial force if the object moves in non-inertial space system. Similarly, partition of the total torque about mass center is

$$\vec{T}_G = \vec{T}_g + \vec{T}_h + \vec{T}_c + \vec{T}_{ni} \quad (14)$$

$\vec{T}_G$ ,  $\vec{T}_g$ ,  $\vec{T}_h$ ,  $\vec{T}_c$  and  $\vec{T}_{ni}$  are the total torque, gravitational torque, hydraulic torque, control torque and non-inertial torque about mass center, respectively.  $\vec{T}_g$  vanishes for 6-DOF motion.

If an object's motion is a rotation about a fixed point, it has three DOF. It is then convenient that the body system is set up with its origin located at the fixed point. Let C denote the fixed point and  $\vec{x}_C$  its position vector in the space system, the coordinate transformation between the space and body systems can be performed using equation (1) with substitution of  $\vec{x}_G$  by  $\vec{x}_C$ . For any point P on the object, its motion is a 3-D rotation about the fixed point and its velocity is written

$$\vec{V}_P = \vec{\omega} \times \vec{r}_{P/C} \quad (15)$$

where  $\vec{r}_{P/C}$  denotes the distance from C to P.  $\vec{\omega}$  is obtained by solving equations (8) in the body system with  $[J]$  denoting the moment of inertia tensor with respect to point C.

Rotation about a fixed axis is a planar motion, which has one DOF only. In this case, the rotation axis must be parallel to one of the three space coordinate axes. The body system is set up with one of its three coordinate axes coinciding with the rotation axis and the other two coordinate axes parallel to those of the space system. Two of the three coordinates of the body system origin are thus the same as those of the rotation axis, and the third coordinate is set equal to zero. For example, if the rotation axis is parallel to the y-axis, and the x- and z-coordinates of the rotation axis are respectively  $x_0$  and  $z_0$ , then the body system ( $x'$ ,  $y'$ ,  $z'$ ) is set up with the  $y'$  axis coinciding with y, while  $x'$  and  $z'$  are parallel to x and z, respectively, and the body system origin is set at  $(x_0, 0, z_0)$ . Angular velocity of the rotating body has only one non-zero component and can be calculated by solving

$$T = J\dot{\omega} \quad (16)$$

where  $T$ ,  $J$  and  $\dot{\omega}$  are total torque, moment of inertia and angular acceleration about the fixed axis in body system. Equation (15) is used to calculate velocity of any point P on the rigid body with C representing any point at the rotation axis.

If a motion is completely user-prescribed, or it is dynamically coupled with fluid flow but its velocity components in one or more directions are user-prescribed, or it is a rotation about a fixed-point or a fixed-axis, then in the directions with prescribed or zero velocity components, the net force and net torque components are calculated from the equations of motion. In this case, the total force and total torque can be different from the total effects of hydraulic, gravitational, non-inertial, and user-prescribed forces and torques, and the differences are called *residual* control force and torque. In other words, both the net control force and the net control torque are divided into two parts: the user-prescribed part and the residual part,

$$F_{c,i} = F_{uc,i} + F_{rc,i} \quad (17)$$

$$T_{c,j} = T_{uc,j} + T_{rc,j} \quad (18)$$

where  $F_{uc,i}$  and  $F_{rc,i}$  are user-prescribed components of control force and residual control force in  $i$ -direction of space system, respectively,  $T_{uc,j}$  and  $T_{rc,j}$  are user-prescribed components of control torque and residual control torque in the  $j$ -direction of body system, respectively. The residual force and torque are calculated by

$$F_{rc,i} = F_i - F_{g,i} - F_{h,i} - F_{uc,i} - F_{ni,i} \quad (19)$$

$$T_{rc,j} = T_j - T_{g,j} - T_{h,j} - T_{uc,j} - T_{ni,j} \quad (20)$$

where the lower index g, h, e, uc and ni represent gravitational, hydraulic, user-prescribed, and non-inertial components, respectively. Examples of residual control force and torque are: for a fixed-axis rotation the axis exerted force and torque on the object to restrict the motion to 1-DOF, and a propulsive force is needed to make a flying object move at a prescribed speed. These forces and torques constitute the residual control forces and residual control torques.

### 3. Modification of Conservation Equations for Fluid Flow

The general form of the continuity equation based on the FAVOR<sup>TM</sup> method is

$$\frac{\partial}{\partial t}(\rho V_f) + \nabla \cdot (\rho \bar{u} A) = S_m \quad (17)$$

where  $S_m$  is a physical mass source term of fluid,  $V_f$  and  $A$  are volume and area fractions. In contrast to stationary object problems,  $V_f$  and  $A$  vary with time in moving object problems and their effects on fluid flow must be considered. Equation (17) can be rewritten

$$\frac{V_f}{\rho} \frac{\partial \rho}{\partial t} + \frac{1}{\rho} \nabla \cdot (\rho \bar{u} A) = -\frac{\partial V_f}{\partial t} + \frac{S_m}{\rho} \quad (18)$$

For incompressible flow, it is reduced to

$$\nabla \cdot (\bar{u} A) = -\frac{\partial V_f}{\partial t} + \frac{S_m}{\rho} \quad (19)$$

Comparing with the continuity equation for stationary object problems,  $-\frac{\partial V_f}{\partial t}$  is equivalent to an additional volume source term. When using the finite volume method, this source term exists only in mesh cells around moving object boundaries. For a first-order approximation in time,  $-\frac{\partial V_f}{\partial t}$  can be discretized into

$$-\frac{\partial V_f}{\partial t} = \frac{V_f^n - V_f^{n-1}}{\delta t} \quad (20)$$

where the upper indices n-1 and n denote the variable values at the previous and current time steps, respectively, and  $\delta t$  is the time difference. Equation (20) is also used in the moving piston model (Sicilian, 1990). For general moving object cases, however, it is difficult to obtain a good mass conservation property using equation (20) due to the

complexity of the object's shape and motion. In this work, a new expression is used for  $-\frac{\partial V_f}{\partial t}$  approximation

$$-\frac{\partial V_f}{\partial t} = \frac{S_{obj}}{V_{cell}} \vec{V}_{obj} \cdot \vec{n} \quad (21)$$

where, as sketched in Figure 1,  $V_{cell}$  is the total volume of the mesh cell,  $S_{obj}$ ,  $\vec{n}$  and  $\vec{V}_{obj}$  are the area, unit normal vector and velocity of moving object boundary in the mesh cell, respectively. Advantages of Equation (21) over (20) are

- 1) (21) is exact in time, but (20) is a first-order approximation.
- 2) (21) possesses good mass conservation property: the net generation of fluid mass over all mesh cells around GMO boundaries is close to zero.
- 3) Programming with (21) is simple because  $S_{obj}$ ,  $\vec{n}$  and  $\vec{V}_{obj}$  can be easily calculated.
- 4) No extra storage for  $V_f^n$  is needed when using (21).

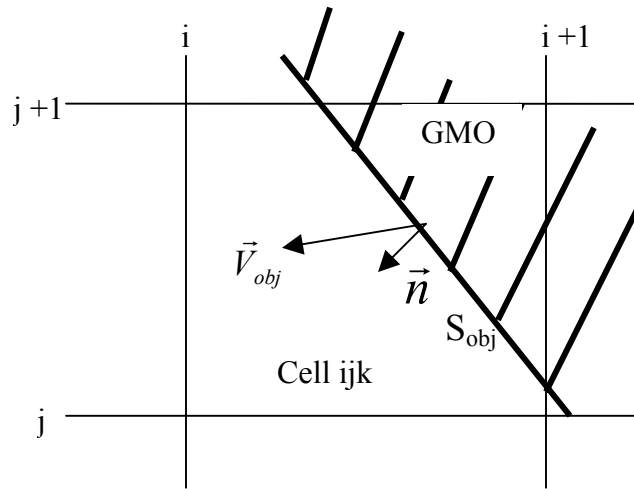


Figure 1. A GMO boundary cell

In FLOW-3D<sup>®</sup>, the momentum equation used is in a non-conservative form, which is obtained by subtracting the continuity equation from the momentum equation in the conservative form. As a result, the terms due to time-change of  $V_F$  are cancelled and the momentum equation in the non-conservative form keeps the same form as that for stationary object problems. Wall shear stress terms in the momentum equations, however, must be modified with consideration of wall motion by using an appropriate tangential velocity. Other transport equations for scalars that are used in their conservative form (*VOF*, energy, etc) are modified by addition of source terms caused by motion of objects.

## 4. Model Implementation

### 4.1 GMO classification

As described in the previous sections, two categories of moving objects are allowed in a multiple GMO system: prescribed motion and fully coupled motion. For the former, in addition to the hydraulic, gravitational and non-inertial forces/torques which are calculated in the solver, a pair of a control force and torque can be prescribed as functions of time either in space or body system. Under each of the two GMO categories, an object can move with six DOF, or rotate about a fixed axis or a fixed point. For a fixed-axis motion, the rotation axis must be parallel to one of the x, y and z coordinate axes of the space system.

There are special cases in which the translational or rotational velocity components of a moving object are prescribed in one or more directions but are dynamically coupled with fluid flow in the other directions. The GMO category is set “coupled” for such moving objects, and several other input parameters must be set to prescribe the user-defined velocity components.

### 4.2 Preprocessor

Moving objects are constructed in the same way as stationary objects except the component copy operation is not allowed. Similarly to stationary objects, a moving object can be composed of a number of subcomponents, and each subcomponent can be defined either by a quadratic function (primitive shape) or by an STL data file. Files with other CAD formats are not allowed to define moving objects. Transformations of a subcomponent is performed in the order of magnification first, then rotation and then translation. Area and volume fractions are split into two parts: the part formed by stationary objects and the part representing moving objects. The former does not change with time thus is calculated in the preprocessor only; the latter, however, varies with time thus is calculated in the solver at each time step. A combination of the two parts in the solver forms the net AF and VF which are functions of time.

In the preprocessor, the body-fixed coordinate system ( $x'$ ,  $y'$ ,  $z'$ ) is set up for each moving object at  $t=0$  with the  $x'$ ,  $y'$ ,  $z'$  axes parallel to the  $x$ ,  $y$ ,  $z$  axes of the space system, respectively. Note that the  $x'$ ,  $y'$  and  $z'$  directions vary with time when  $t > 0$  due to the object's motion. The origin of the body system is set at the GMO's mass center for 6-DOF motion, at the fixed point for a fixed-point rotation, and at a point on the rotation axis for a fixed-axis rotation, as mentioned previously in section 2. Note that only two of the three coordinates of the system origin are needed as input data for the fixed-axis motion, and the code automatically sets the third coordinate equal to zero.

For a motion with six DOF, location and orientation of the GMO at any time are described by its mass center coordinates in space system and the transformation tensor between the space and the body systems. If an object's motion is a rotation about a fixed axis or a fixed point, the object's location is fixed but its orientation varies with time and is also described by the transformation tensor. The transformation tensors for all moving objects are initialized as unit tensors in the preprocessor.

A 6-DOF motion is described by a translational velocity of its mass center and an angular velocity of the object. If a motion has a fixed axis or a fixed point, then it is described by the angular velocity only. Note that the translational velocity components are always defined in the space system, while the angular velocity components are defined in the body system.

For prescribed 6-DOF motion, users must input the mass center velocity components in space system and the angular velocity components in body system, each as a function of time. For prescribed motion with a fixed-point or a fixed-axis, only the relevant components of the angular velocity need be defined. Default values of prescribed velocity components are constantly zero.

Initial translational and rotational velocity components need be given as input for a coupled 6-DOF motion. For a coupled fixed-axis motion and a coupled fixed-point motion, it is required to input the initial values of the relevant rotational velocity components. Default values of all initial velocity components are zero. Note that there can be special cases in which translational or rotational velocities of a moving object are prescribed in one or more directions but are coupled with fluid flow in the other directions. This type of moving objects is categorized as coupled motion, and time-variations of the prescribed velocity components need be defined. Control force and torque can be prescribed in all available directions in either space system or body system for couple motion.

For a GMO with coupled motion, inertia parameters must be given fully in the input file since no physically meaningful default values are available. There are two options for inertia data input. The first option is to give the total mass, the initial mass center coordinates in space system and moment of inertia tensor about mass center (for 6 DOF motion) or about the fixed-point (for fixed point motion) in body system. For fixed-axis motion, rather than giving the inertia tensor, users only need to provide moment of inertia about the fixed-axis. The second option is to provide only the mass density of the moving object. In the latter case the object must be initially located inside the computational domain completely so that the total mass, initial mass center location and moment of inertia tensor can be calculated in the preprocessor based on the uniform density assumption. If multiple GMOs exist, each GMO can have its own inertia data input. For GMOs with prescribed motion, input of the inertia data is not required but is optional: if it is provided using either of the two options, then the residual control force and torque will be calculated by the solver and output as history data.

### **4.3 Solver**

At the beginning of each time step - before flow is calculated - the following variables related to each GMO are calculated explicitly:

- 1) Mass center locations (if needed) and object orientations.
- 2) Volume and area fractions and related variables.
- 3) Mass center velocities (if needed) and angular velocities.

- 4) Hydraulic, gravitational, non-inertial and control forces and torques (if any needed).
- 5) Source term in continuity equation due to the object's motion.

The forces and torques are calculated starting with the second time cycle of a computation because, if the initial pressure distribution is not given accurately, computational instabilities may result.

The mass center velocity and the angular velocity of a GMO are calculated by solving equations of motion in space and body systems, respectively, as presented in section 2. The transformation tensor which describes object's orientation is calculated by solving its time-dependent differential equation (4). The mass center location is obtained by integrating the mass center velocity for a 6-DOF motion. For fixed-axis and fixed-point motions, it is obtained through coordinate transformation between space and body systems using the transformation tensor. The rotation angle for a fixed-axis motion is also calculated from the transformation tensor. Based on the right-hand convention, the positive direction of rotation is the same as that of the coordinate axis which the rotation axis is parallel to. If the maximum and the minimum rotation angles are given in input, then the rotation will be restricted to be within the two limits.

There are two basic effects of an object's surface motion on fluid flow: 1) the normal component of the surface velocity displaces fluid through pressure increase/decrease, and 2) the tangential component affects the flow through wall shear stress. The first effect is accounted by addition of the source term in the continuity equation, which is calculated at each time step using equation (21). The second effect is considered by modifying the shear stress terms in the momentum equations using a non-zero wall velocity.

#### ***4.4 Output data lists***

The following variables are computed and stored in the main data file (flsgrf.\*) and can be available for post-processing for each moving object:

- Mass center coordinates in space system.
  - Mass center velocity in space system.
  - Angular velocity in body system.
- Hydraulic force in space system.
- Hydraulic torque about mass center, fixed-axis or fixed-point in body system.
- Residual control force and torque in space and body systems if they exist.
- Rotational angle for fixed-axis rotation.

The availability of output of these variables depends on what type of motion the moving object possesses.

## **5. Model Application and Validation**

In this section the fixed-mesh method for GMO (the GMO model) is illustrated by its application to several problems. The capabilities of the model for prescribed and coupled

6-DOF motions, fixed-axis rotations and fixed-point rotations are presented. Validation is made for some simple cases.

### 5.1. Buoyancy Force on a Stagnant Sphere in Static Water

Buoyancy force on a stagnant sphere in water was calculated and compared with the theoretical result of the Archimedes' Law. A 1.0 m diameter sphere was centered in a 2m×2m×2m tank with water depth of 1.8 m. Computations with different mesh sizes were carried out using the GMO model and are listed in Table 1. Theoretical value of buoyancy is 5131.3 N. It can be seen that the model gives good accuracy for prediction of the buoyancy force, and the accuracy increased rapidly with increasing mesh resolution. This implies that the pressure force calculation in the model gives accurate results.

**Table 1.** Comparison of calculated and theoretical buoyancy forces for a 1.0 m diameter sphere in static water (Theoretical value is 5131.3 N)

Number of Mesh Cells	Buoyancy (N)	Error
20×20×20	5062.5	1.34%
40×40×40	5116.4	0.290%
80×80×80	5130.7	0.0117%

### 5.2 Magnus Force on a Rotating Sphere

The Magnus force is defined as the lift force on an object (*e.g.*, sphere and cylinder) rotating in a stream about an axis perpendicular to the stream. The cause of the lift force is mainly the pressure difference at two sides of the object resulting from the velocity difference due to object rotation. Using the GMO model and the multi-block technique, the Magnus force on a rotating sphere in an air stream was calculated and compared with the measurements of Barkla *et al* (1971). The sphere was 6.4 cm in diameter and rotated at 800 rotations per minute about an axis perpendicular to the stream. Physical time was 5.0 sec. The ratio of the sphere's peripheral velocity to air stream velocity was 5.0. Figure 1 shows the steady-state pressure and velocity vector distributions around the sphere. The pressure was lower at the upper side than the lower side of the sphere due to the velocity difference, causing an upward lift force (the Magnus force).

The lift force is expressed in the form based on a dimensional analysis

$$L = \frac{1}{2} \rho C_L S U_0^2$$

where  $S$  is the projected area of the sphere,  $U_0$  is air stream velocity,  $\rho$  is air density, and  $C_L$  is the lift force coefficient. From the calculated lift force  $3.40 \times 10^{-4}$  N, the coefficient  $C_L$  was obtained as 0.60, while the measured  $C_L$  value by Barkla *et al* (1971) is 0.5.

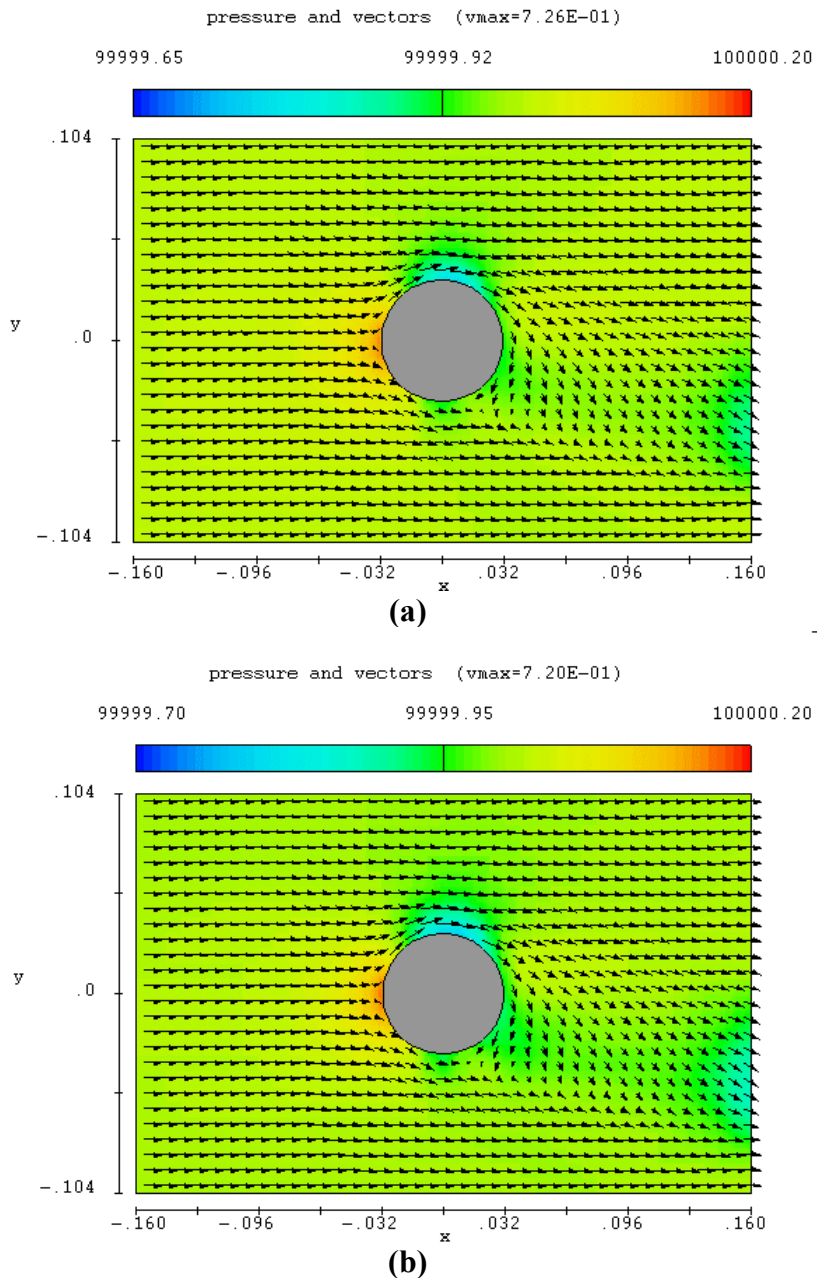


**Figure 2.** Comparison of velocity and pressure distributions in center plane by GMO model and axisymmetric rotating object model. (a) GMO model, (b) axisymmetric rotating object model.

To further evaluate the general moving object model, the computation was repeated using the old model of *FLOW-3D* for axisymmetric rotating objects. The calculated lift force includes the effects of both pressure and shear stress. A comparison of the computational results by the two models and the experimental result are presented in Table 2. Figure 2 shows a comparison of the velocity and pressure distributions in the center plane for both computations at steady state. The results of the two models are very close, implying that the computation using the GMO model yields similar accuracy to

that using axisymmetric rotating object technique. Although the GMO model calculates area and volume fractions at each time step, it used only 13% more CPU time and 3.6% more cycles (or timesteps) than the asymmetric rotating object technique.

**Table 2.** Comparison of computations and experiment for Magnus force

	GMO model	Asymmetric rotating object capability	Experiment by Barkla et al (1971)
$C_L$	0.600	0.584	0.5
CPU Time (s)	25350	22400	—
Total no. of cycles (time steps)	4365	4212	—

### 5.3 Shot sleeve simulation

The operation of a shot sleeve was simulated using the GMO model and compared with the result of the existing moving piston model of *FLOW-3D*<sup>®</sup>. Figure 3 shows liquid metal at different time instants. A pressure boundary condition was used at the exit hole. Piston motion was prescribed with the initial speed of 15.24 cm/s which is much slower than surface wave speed. At  $t=0.67$  s, the piston's speed was increased to 57.66 cm/s which is higher than surface wave speed, resulting in a pileup of liquid metal at the piston surface. Liquid metal continued to pile up in front of the piston until it fully occupies the sleeve space and exited through the upper opening at the end of the sleeve. Figure 4 shows the change of volume with time (curve 2) and its comparison with the result of the old piston model (curve 1). The GMO model maintained a nearly constant volume of fluid before liquid metal leaves the sleeve at about 2.6 s. The old model, however, yields a 15% unphysical increase of the fluid volume. This indicates that the GMO model is a significant improvement over the old model with regards to the mass conservation property due to the usage of the new expression of source term in the continuity equation, as discussed in Section 3.

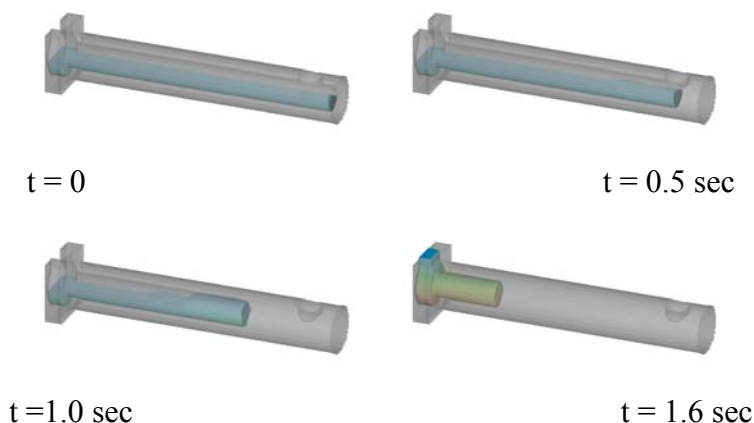


**Figure 3.** Liquid metal at different times.

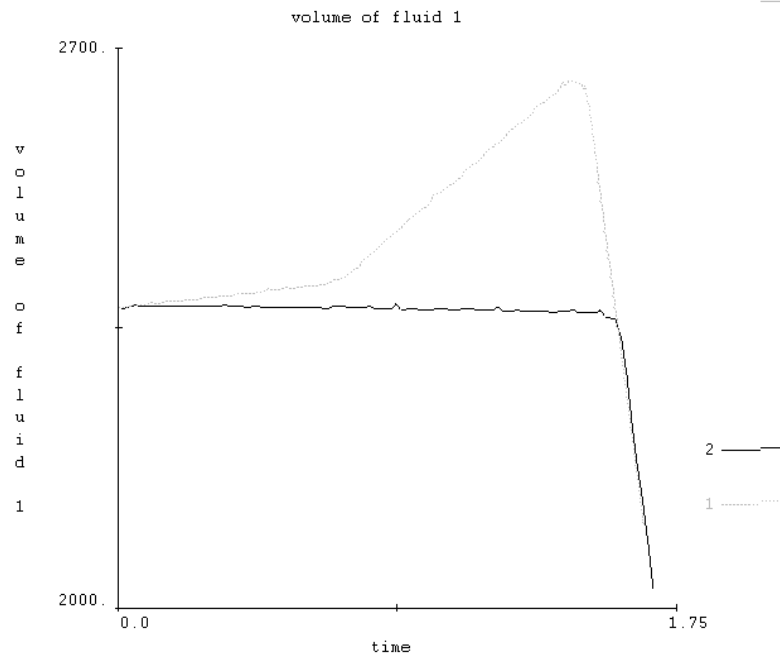


**Figure 4.** Volume of fluid vs time. Curve 1: old moving object model. Curve 2: the GMO model

#### 5.4. Pendulum motion

A test was conducted for a physical pendulum illustrated in Figure 5, which was a 0.1 m×0.4 m×0.1 m rectangular prism swinging freely about a fixed point at its end. There was no fluid in this simulation. Mass density of the pendulum was set at 800 kg/m<sup>3</sup>. The computational domain was 1m×0.2m×0.6m with a uniform 50×10×50 mesh. The pendulum was released from the initial location at the 45° angle from vertical line. The physical time was 3 sec, and the time step size was fixed at 0.01 sec. This case was designed to test the rigid body dynamics of the GMO model by comparing computational and theoretical results. Figure 6 shows the variation of the rotational angle and angular velocity of the pendulum with time, which are sine curves as is analytically derived. Table 3 shows the calculated moment of inertia about the rotation axis and period with their comparisons with theoretical results. From rigid body dynamics, the period of oscillation of the pendulum is

$$T = 2\pi \sqrt{\frac{J_o}{mgL}} \quad (22)$$

where  $J_o$  is the moment of inertia about the rotation axis,  $L$  is the distance from the mass center to the rotation axis,  $m$  is the mass of the pendulum, and  $G$  is the gravitational

acceleration. The calculated moment of inertia and period have errors of 6.1% and 2.8% relative to the theory, indicating a reasonable match.

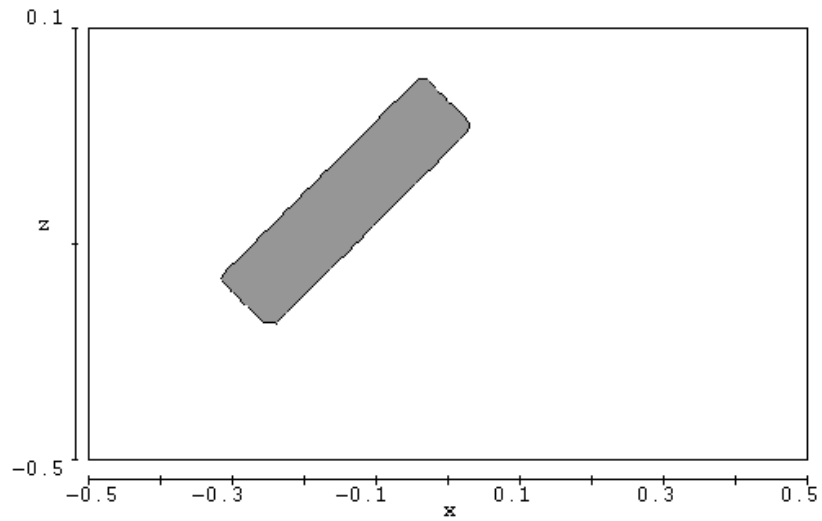
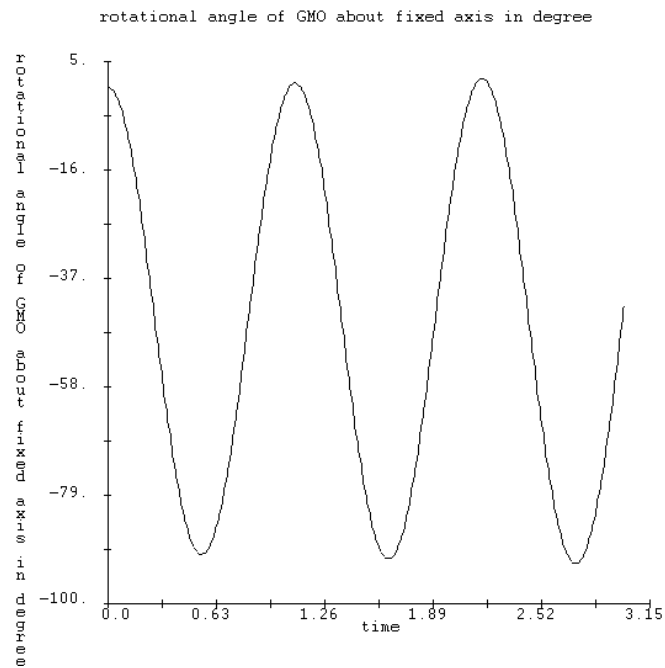
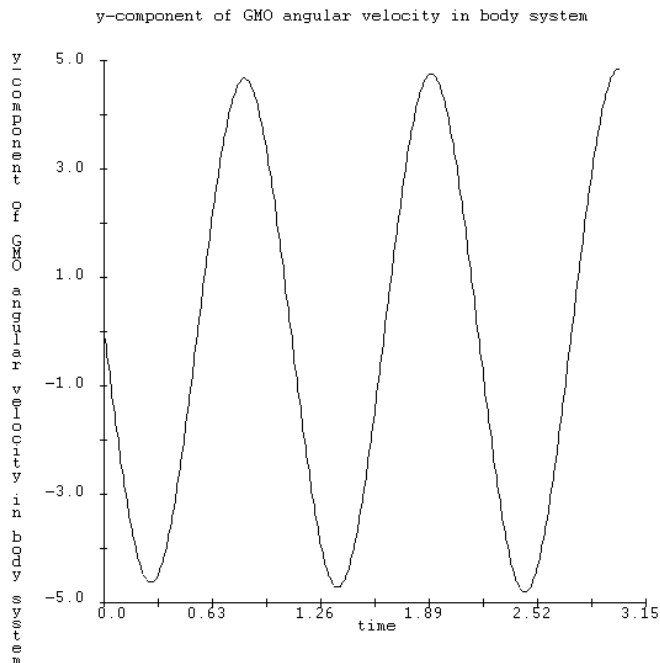


Figure 5. Illustration of pendulum at its initial position.





(b)

**Figure 6.** Variations of the rotation angle and angular velocity of the pendulum with time: (a) rotation angle, (b) angular velocity

**Table 3.** Comparison between the computation and theory for the pendulum motion

	Computation	Theory
Moment of inertia ( $\text{kgm}^2$ )	0.170	0.181
Period (s)	1.09	1.07

### 5.6 Valve opening

A prediction of the opening of a spring-loaded valve in a pipe at different flow rates was conducted. Figure 7 shows the initial location of the valve piston and the non-uniform mesh around it. Water flowed in the negative  $z$  direction, which is down on the images. A spring (not included explicitly in the geometry) under the piston is compressed when the valve opens, providing a resistance force against valve opening. A three-dimensional computational domain was defined from  $z = -52$  cm to 62 cm, which is longer than what is shown in Figure 7. The total number of mesh cells was approximately 178,000. In the experiment, the flow rate was increased from 0 to 50, to 125, 180, 250, 325, 400, 450, 500 and 550 gal/min step by step. In the computation, the flow rate increased linearly from one flow rate value to the next within one second, remained constant for another second, and then increased linearly to the next value, until it reached 550 gal/min. An RNG turbulence model was used in the calculation. Figure 8 shows two predicted

positions of the valve piston and the corresponding velocity vector distributions. Figure 9 shows a comparison between the predicted and measured piston positions at different flow rates. The prediction matches the experimental result very well at flow rates less than 300 gal/min. The piston was opened completely at about 350 gal/min in the prediction, but in the experiment it stopped moving at 340 to 460 gal/min and was completely open at 500 gal/min. One possible reason for this mismatch is that cavitation bubbles might have been present in the experiment at high flow rates, which would have reduced the pressure drop around the valve, causing a smaller drag force on the piston than that predicted by the model.

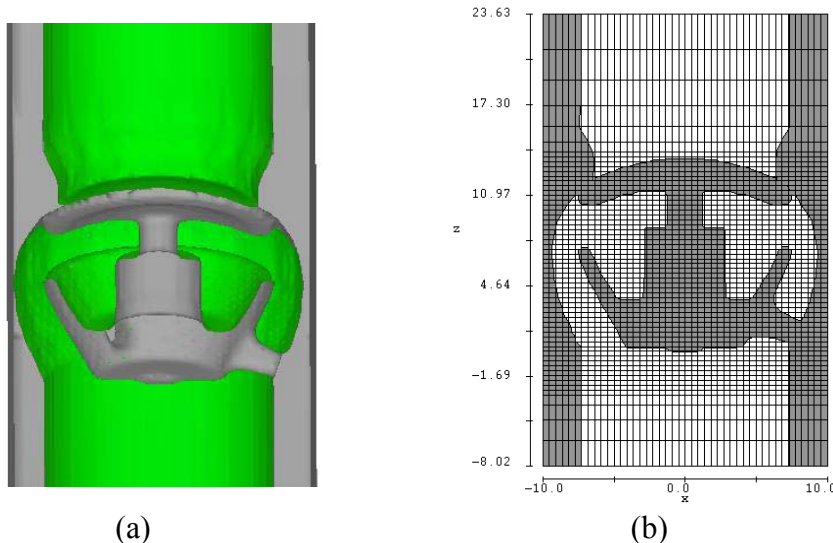


Figure 7. Geometry and mesh around the valve piston. (a) Geometry at  $t=0$ , (b) mesh in  $x$ - $z$  plane ( $x$  and  $z$  in cm).

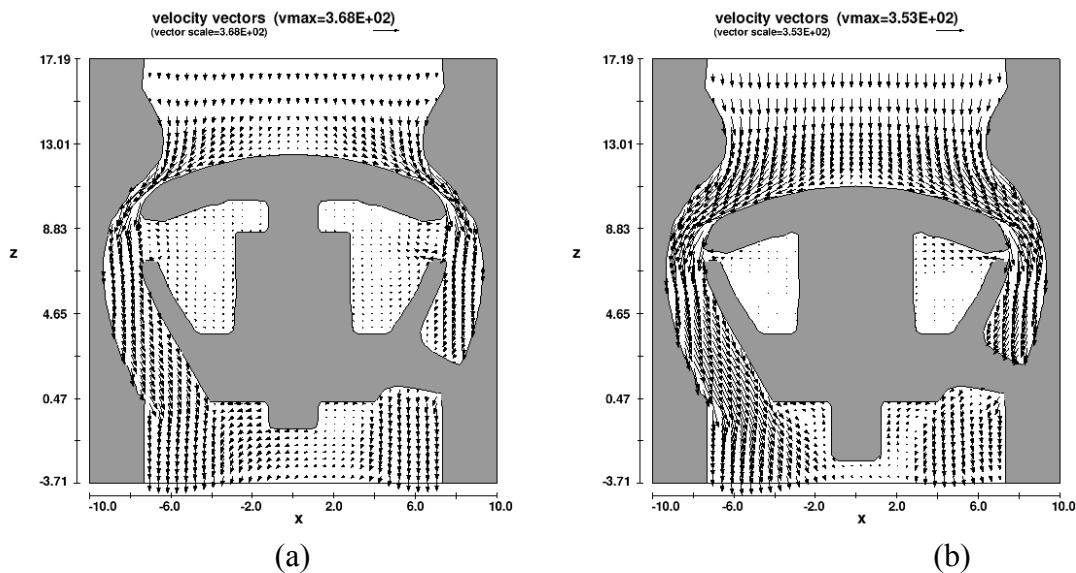


Figure 8. Valve piston location with pressure and velocity vector distributions at (a)  $t=0.6$  s and (b)  $t=1.5$  s.

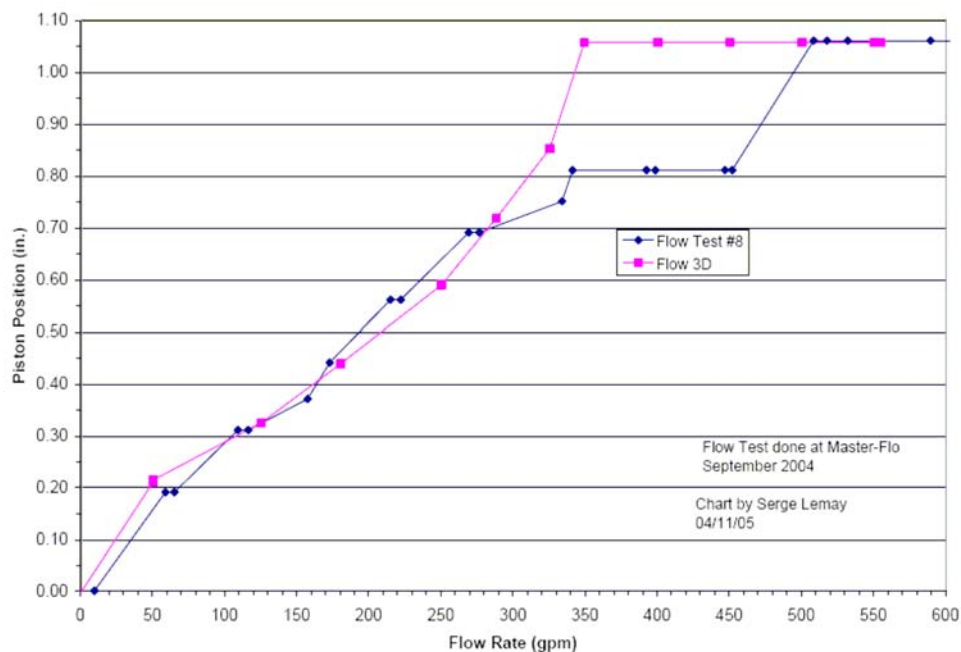


Figure 9. Predicted and measured valve piston positions at different flow rates  
(*Courtesy of Stream-flo Industries Ltd*)

### 5.7 Entry of a sphere into water

The last test involved a more dynamic interaction of a rigid body with water. An aluminum sphere,  $0.099\text{ m}$  in diameter, was dropped vertically into a large quiescent pool of water with an initial speed of  $8.8\text{ m/sec}$ . The projectile penetrates deep into the water, creating an air cavity in its wake as shown in Fig. 10(a) (Batchelor, 1967).

The flow was modeled using the GMO model for coupled motion in a three-dimensional rectangular mesh with a uniform grid spacing of  $0.006\text{ m}$ . The results are shown in Fig. 10. The images in the simulation were chosen at the times when the penetration depth of the sphere approximately matched the three experimental images. The model predicts a somewhat smaller size of the upper cavity. The separation of the air cavity behind the sphere into two smaller cavities in the model occurs at a similar depth as in the experiment. The size and shape of the secondary air cavity right behind the sphere is also reasonably close to the experiment. The computed variation of the vertical component of the projectile's velocity shows that, despite the shortness of the time, it underwent a change of around 12% of the initial value.

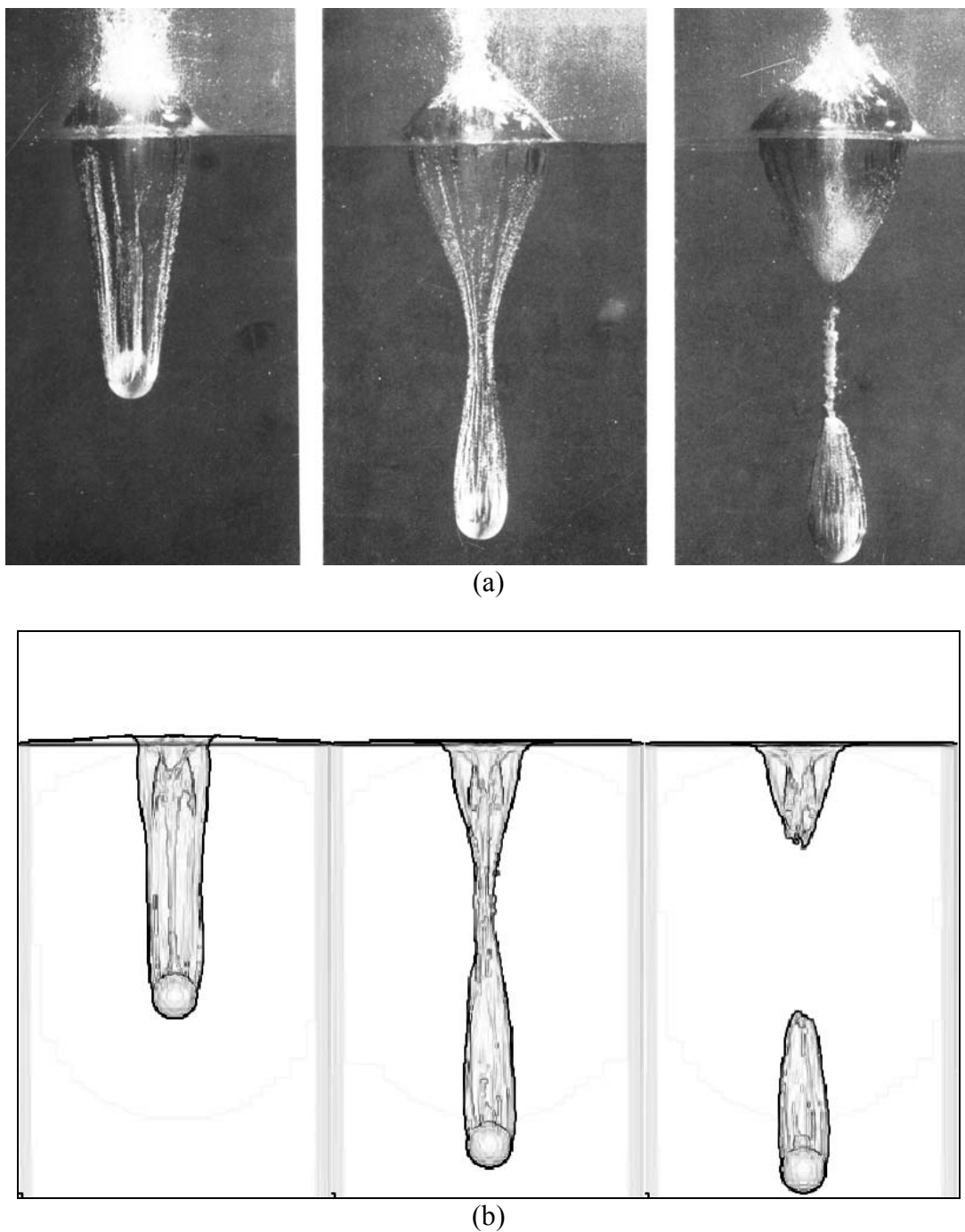


Figure 10. Cavity formed during entry of a sphere of diameter  $0.099\text{ m}$  into water at a speed of  $8.8\text{ m/sec}$ . Experimental results in (a) were taken from Batchelor (1967). The simulation images in (b) show the bubble trail behind the sphere roughly at the same times as the experiment.

## 6. Conclusions

A fixed-mesh method for general moving objects (GMO) in fluid flow based on the FAVOR<sup>TM</sup> technique was developed and implemented in a commercial CFD package **FLOW-3D**<sup>®</sup>. A GMO is a rigid body with any type of six-degrees-of-freedom, fixed-point or fixed-axis motion which can be either user-prescribed or dynamically coupled to fluid flow. For coupled motion, part of its velocity components can be user-prescribed while the others remain coupled. The method allows multiple general moving objects, and each of them can be assigned any of these types of motion. At each time step, area and volume fractions in a fixed-rectangular mesh are calculated to describe the object's motion. Hydraulic, gravitational, environmental, non-inertial and residual control forces and torques are calculated for each moving object, and rigid body equations of motion are solved explicitly for translational and rotational velocities for objects under coupled motion. The continuity equation is modified with the addition of a source term to account for the effect of moving objects on fluid. The wall shear terms in the momentum equations are also modified accordingly. This method has distinct advantages over the moving and deforming mesh methods because it treats complex moving object geometries very efficiently and conveniently and there is no restriction on closeness between objects or the complexity of the motion itself. Good agreements are achieved between computational and theoretical/experimental results in several application cases.

## Reference

- Batchelor G. K., 1967, An Introduction to Fluid Dynamics, Cambridge, Cambridge University Press.
- Barkla H. M. and Auchterlonie, 1971, The Magnus or Robbins Effect on Rotating Spheres, J. Fluid Mech., vol. 47, part 3, 437-447.
- Crank J., 1984, Free and Moving Boundary Problems, Oxford, Oxford University Press.
- Ditter J.L. and Hirt C.W., 1993, A Scalable Model for Stir Tanks, Technical Note #38 (FSI-93-TN38), Flow Science, Inc.
- Finlayson B. A., 1992, Numerical Methods for Problems with Moving Fronts, Ravenna Park Publishing, Ravenna Park, WA.
- Goldstein H., Charles P. and Safko J., 2002, Classical Mechanics, Addison Wesley, Washington.
- Hirt C. W. and Sicilian J. M., 1985, A Porosity Technique for the Definition of Obstacles in Rectangular Cell Meshes, Proc. Fourth International Conf. Ship Hydro., National Academic of Science, Washington, DC.
- Sicilian J. M., 1990, A FAVOR<sup>TM</sup> Based Moving Obstacle Treatment for FLOW-3D. Technical Note #23 (FSI-90-TN23), Flow Science, Inc.